XIX IMEKO World Congress
Fundamental and Applied Metrology
September 6−11, 2009, Lisbon, Portugal

STUDY OF THE INFLUENCE OF CONVECTIVE EFFECTS IN INCIDENT RADIATIVE HEAT FLUX DENSITY MEASUREMENT UNCERTAINTY

L. Lages Martins, A. Silva Ribeiro and C. Pina dos Santos

Laboratório Nacional de Engenharia Civil, Lisbon, Portugal
lfmartins@lnec.pt, asribeiro@lnec.pt, pina.santos@lnec.pt

Abstract – This study describes the measurement uncertainty propagation of the incident radiative heat flux density quantity associated with different exposure conditions of the heat flux meter, taking into account the convective effects in reaction to fire tests.

To accomplish this aim, considering the complexity and non-linearity of the applied mathematical models to perform the indirect measurement of the above mentioned quantity, the Monte Carlo method was applied.

The use of this numerical approach allows to estimate the quality of the measurements within a high accuracy level and to evaluate deviations related with the GUM method since it provides an approximate solution for this specific metrological problem.

The experimental examples presented concern to the reaction to fire testing (the room-corner test and the flooring radiant panel test) with different exposure conditions of the heat flux meter used, being the applied mathematical model described on each case and a sensitivity analysis of the input uncertainty contributions presented.

Keywords: incident radiative heat flux density; measurement uncertainty; Monte Carlo method.

1. INTRODUCTION

The measurand incident radiative heat flux density has an important role in reaction to fire testing being applied in the room-corner test [1] and in the flooring radiant panel test [2], where it is the most significant heat transfer mode that occurs in a fire. In these tests, the estimate of this physical quantity allows the evaluation of the tested materials contribution to fire deflagration and propagation.

In the mentioned reaction to fire tests, this thermal quantity is indirectly measured using an appropriate mathematical model derived from the energy balance performed at the surface of the heat flux meter used [3]. The focus of this study was on the Schmidt-Boelter heat flux meter performance, one of the most common used in reaction to fire testing laboratories, such as the *Laboratório de Ensaios de Reacção ao Fogo* at the *Laboratório Nacional de Engenharia Civil* (LNEC/LERF) which supported the experimental work.

The equipment used is unable to perform direct measurement of the incident radiative heat flux density component, due to the combined effects of radiation and convection, despite some attempts to reduce the convective effect. One of these attempts consisted in the use of glass windows connected to the heat flux meter, considered inappropriate due to the output measurement uncertainty increase related with additional uncertainty contribution of the optical properties [4].

Considering the non-linear mathematical model used to obtain the incident radiative heat flux density by an indirect measurement and the need to account for the convective effects, the study carried out intended to evaluate the propagation of the measurement uncertainty using the Monte Carlo method (MCM) [5] specially suited to this type of problem.

In order to discuss this approach, two experimental conditions were studied: the room-corner fire test, in which the heat flux meter sensor head (with a cylindrical shape) is totally exposed to the air flow (figure 1.a); and the radiant panel fire test, in which only the top sensor surface is exposed to the air flow (figure 1.b).

Since the air flow over the top surface of the sensor depends on the exposure condition, the convective heat transfer will also be different and, therefore, it should be accounted for in the mathematical model presented in section 2.

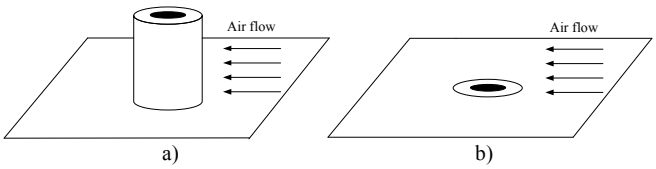

Figure 1. Different exposure conditions of the heat flux meter sensor head.

For both studied conditions, the MCM approach provides information to perform a measurement uncertainty sensitivity analysis, obtained by introducing independent incremental changes on each input measurement uncertainty and evaluating the corresponding output measurement uncertainty variation. The applied increment is defined in order to produce an output variation with a higher magnitude than the computational accuracy level of the performed numerical simulations.

ISBN 978-963-88410-0-1

2. INCIDENT RADIATIVE HEAT FLUX DENSITY MEASUREMENT MODEL

The establishment of the incident radiative heat flux density measurement model implies performing an energy balance of the different heat transfer modes at the surface of the heat flux meter sensor head.

Figure 2 represents the surface and the control volume in which it is possible to identify the following heat transfer modes and corresponding heat flux densities:

- incident radiation, $\varphi_{\text{rad, inc}}$, generated by high temperature of the surrounding elements due to the reaction to fire test;
- reflected and emitted radiation by the surface of the heat flux meter sensor head, $\varphi_{\text{rad, ref}}$ and $\varphi_{\text{rad, em}}$, respectively;
- convection on the sensor surface, φ_{conv}, generated by the air flow with temperature T_∞ and velocity u_∞;
- conduction, φ_{cond}, from the warm external surface to the cooled inner core.

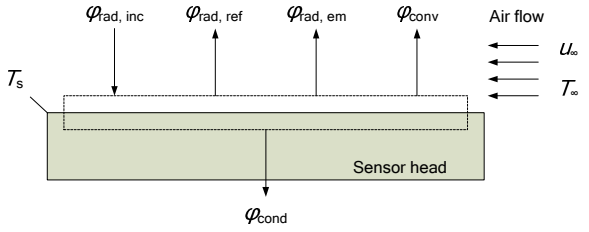

Figure 2. Diagram of energy flux transfer at the sensor head and measurement influence quantities.

Assuming a steady-state condition, the energy balance can be expressed by the following mathematical model (the output quantity is the incident radiative heat flux density):

$$\varphi_{\text{rad, inc}} = \varphi_{\text{rad, ref}} + \varphi_{\text{rad, em}} + \varphi_{\text{cond}} + \varphi_{\text{conv}} . \quad (1)$$

In the evaluation of the other radiative terms, the surface of the sensor head is considered diffuse and grey, i.e, the surface's absorptivity and emissivity are taken as independent from the radiation direction and wavelength. This assumption allows to establish an equivalence between the surface's emissivity, ε_s, and absorptivity, α_s, being the reflected radiation heat flux density given by

$$\varphi_{\text{rad, ref}} = (1-\varepsilon_s)\,\varphi_{\text{rad, inc}} , \quad (2)$$

and the emitted radiation heat flux density

$$\varphi_{\text{rad, em}} = \varepsilon_s\, \sigma\, T_s^4 , \quad (3)$$

where σ is the Stefan-Boltzmann constant and T_s is the surface temperature of the heat flux meter sensor head.

The evaluation of the conduction heat flux density estimate is obtained using expression (1) being based on the heat flux meter calibration. The LNEC/LERF heat flux meter is calibrated by the spherical black-body cavity method, according with ISO 14934-2 (2006). This method establishes a procedure of decreasing the convective effect on the heat flux meter to a minimum in such a way that it can be considered neglectable. In this condition, the energy balance can be given by the following expression

$$\varphi_{\text{rad, inc}} = \varphi_{\text{rad, ref}} + \varphi_{\text{rad, em}} + \varphi_{\text{cond}} . \quad (4)$$

The calibration provides data that can be used to determine a linear relation between the incident radiative heat flux density and the heat flux meter output electric tension, V,

$$\varphi_{\text{rad, inc}} = C\, V , \quad (5)$$

where C is the calibration constant.

Applying the previous expression together with expressions (2) and (3) to the energy balance, expression (5) allows to write the conduction heat flux density as

$$\varphi_{\text{cond}} = \varepsilon_s \left(C\, V - \sigma\, T_{s,\text{cal}}^4\right), \quad (6)$$

in which $T_{s,\text{cal}}$ corresponds to sensor head surface temperature during calibration.

The convective term presented in expression (1) can be expressed in general as

$$\varphi_{\text{conv}} = \bar{h}\left(T_s - T_\infty\right), \quad (7)$$

where $\bar{h}$ is the average convection heat transfer coefficient, being dependent on several parameters such as the surface geometry, the nature of the air flow (laminar or turbulent) and its thermophysical properties.

For both exposure conditions studied (displayed on figure 1), laminar air flow was considered and the thermophysical properties of the air flow refers to the film temperature (average temperature between the air flow temperature and the surface temperature of the heat flux meter sensor head). However, the surface geometry is different in each case, requiring the use of adequate convection coefficients.

According to [4], a reasonable coefficient estimate for the first exposure condition corresponds to

$$\bar{h} = \frac{0{,}24\, u_\infty^{\frac{2}{3}}\, k}{\nu^{\frac{2}{3}}\, d^{\frac{1}{3}}} , \quad (8)$$

where k and ν are the air flow thermal conductivity and the cinematic viscosity at film temperature, respectively, and d is the sensor head diameter.

For the second exposure condition, the flat plate approach was considered and, according to [6], the average convection heat transfer coefficient in a laminar flow is given by

$$\bar{h} = \frac{0{,}664\, Re^{\frac{1}{2}}\, Pr^{\frac{1}{3}}\, k}{d} , \quad (9)$$

being Re the Reynolds number and Pr the Prandtl number. This expression is valid only for $0{,}6 \le Pr \le 50$.

Introducing the previous deducted expressions of the heat flux density terms into expression (1), the incident radiative heat flux density measurement model for the first exposure condition becomes

$$\phi_{\text{rad,inc}} = \frac{1}{\varepsilon_s}\left[\frac{0{,}24\,u_\infty^{\frac{2}{3}}\,k}{\nu^{\frac{2}{3}}d^{\frac{1}{3}}}\left(T_s - T_\infty\right) + \varepsilon_s\,\sigma\left(T_s^4 - T_{s,\text{cal}}^4\right) + \varepsilon_s\,CV\right], \quad (10)$$

and for the second exposure condition

$$\phi_{\text{rad,inc}} = \frac{1}{\varepsilon_s}\left[\frac{0{,}664\,Re^{\frac{1}{2}}Pr^{\frac{1}{3}}k}{d}\left(T_s - T_\infty\right) + \varepsilon_s\,\sigma\left(T_s^4 - T_{s,\text{cal}}^4\right) + \varepsilon_s\,CV\right]. \quad (11)$$

3. EVALUATION OF THE MEASUREMENT UNCERTAINTY

3.1 Probabilistic framework and calculation method

The above mathematical models (10) and (11) share almost all of the input quantities. In fact, the only exception is the Prandtl number, applied only in (11), considering that the Reynolds number can be obtained as a function of u_∞, d and ν. Therefore, both models can be illustrated by the same functional diagram exhibited in following figure.

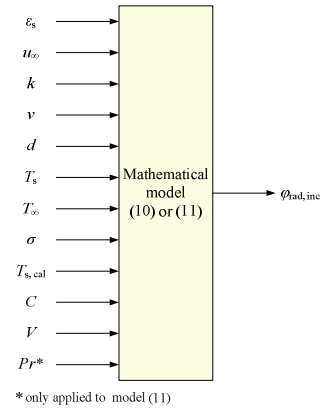

Figure 3. Functional diagram for the two exposure conditions.

Regarding the exposition condition related with the room-corner test (figure 1.a), the probabilistic framework of the input quantities used in the MCM simulation (Table 1) is similar to the one adopted in [4] which follows the conventional GUM approach. The use of the same probabilistic assumptions allows a direct comparison between the evaluated measurement uncertainties obtained using both methods.

Several input estimates related with the heat flux meter output electric tension were studied in order to know the behaviour of the output quantity measurement uncertainty – incident radiative heat flux density – considering the nominal measuring interval of, approx., 2 kW·m^{-2} to 20 kW·m^{-2}. This interval comprehends the incident radiative heat flux estimates usually obtained in the room-corner test.

The study of convective effects influence was developed using different estimates for the air flow temperature (from 289 K to 337 K) and for the air flow velocity (from 0,3 m·s^{-1} to 1,3 m·s^{-1}). Again, the same conditions adopted in [4] were considered, namely, the probability density functions (PDF) are all gaussian and the measurement uncertainties of d, k, ν and σ are assumed to be neglectable within this framework.

Table 1. Probabilistic framework related with the input quantities in the room-corner test [4].

Input quantity	Estimates	PDF	Relative standard uncertainty
ε_s	0,96	gaussian	±3 %
C (W·m^{-2}·mV^{-1})	5132		±3 %
V (mV)	0,5; 1,0; 2,0; 3,0; 4,0		±0,5 %
$T_{s,cal}$ (K)	295		±1 %
T_s (K)	297		±2 %
u_∞ (m·s^{-1})	0,3; 0,6; 0,9; 1,3		±20 %
T_∞ (K)	289; 320; 337		±10 %
d (m)	0,025	-	-
k (W·m^{-1}·K^{-1})*	26,3 x 10^{-3}	-	-
ν (m^2·s^{-1})*	15,89 x 10^{-6}	-	-
σ (W·m^{-2}·K^{-4})	5,670 x 10^{-8}	-	-

* Estimates for a film temperature equal to 300 K.

For the exposition condition related with the radiant panel test (figure 1.b), the input data was the one available at LNEC/LERF regarding the heat flux meter used (specially, the technical specifications and the calibration certificates) and the results obtained from the following experimental tests:

- surface temperature – the use of a non-contact infrared thermometer has revealed that the surface temperature estimates on the heat flux meter sensor head (at the several reference positions and after establishing a steady-state condition) can change from 390 K to 480 K; the measurement uncertainty was estimated to be within ±2 K (based on technical specifications);
- air flow velocity – several attempts were made in order to measure the air flow velocity inside the test chamber (with the ventilation system activated and in the absence of combustion, since available measurement instruments such as the hot wire anemometer or the turbine anemometer can not withstand high temperatures); the obtained estimates were equal to zero for all reference measuring positions, considering a instrument resolution equal to 0,1 m·s^{-1}; with the presence of combustion at the radiant panel it is expected that, due to the temperature gradient and, consequently, the air density gradient, free convection will occur and the air flow velocity will not be equal to zero; due to the lack of consistent experimental data, the probabilistic formulation for this quantity is considered to be identical to the one mentioned for the room-corner test (see table 1) in [4];

- air flow temperature – the LNEC/LERF test chamber has a thermocouple at its upper part intended to measure air temperature inside the chamber; experimental data related with this measurand shows that the air temperature in this region can rise up to 400 K (≈ 127 ºC) with a experimental standard deviation of ±8 K; since the measurement of heat flux density is performed at the lower part of the test chamber, close to the air inlet (usually the ambient temperature is near 300 K, i.e., 27 ºC), it is considered that the input temperature estimate can change between 300 K and 400 K and that the measurement uncertainty is given by the above experimental standard deviation.

Taking into account the estimates of T_s and T_∞, the film temperature can change between 350 K and 450 K and the thermophysical properties of the air flow will change accordingly. For this reason, the probabilistic formulation of k, Pr and ν is based on uniform PDFs in which all thermophysical properties values [6] between 350 K and 450 K are considered equally probable.

Table 2 summarizes the probabilistic information of the several accounted input variables used in the development of MCM calculation stage.

Table 2. Probabilistic description of the input quantities in the flooring radiant panel test.

Input quantity	Estimates	PDF	Standard uncertainty
ε_s	0,945	uniform	± 0,003
C ($W \cdot m^{-2} \cdot mV^{-1}$)	553,5	gaussian	± 1,5 %
V (mV)	2; 4; 6		± 0,004
$T_{s,cal}$ (K)*	295		± 3
T_s (K)	390; 450; 480		± 2
u_∞ ($m \cdot s^{-1}$)	0,3; 0,6; 0,9		± 20 %
T_∞ (K)	300; 350; 400		± 8
d (m)	0,025 00		± 0,000 02
k ($W \cdot m^{-1} \cdot K^{-1}$)	$33{,}9 \times 10^{-3}$	uniform	$\pm 2{,}2 \times 10^{-3}$
Pr	0,693		± 0,004
ν ($m^2 \cdot s^{-1}$)	$26{,}7 \times 10^{-6}$		$\pm 3{,}3 \times 10^{-6}$
σ ($W \cdot m^{-2} \cdot K^{-4}$)**	$5{,}670\,4 \times 10^{-8}$	gaussian	$\pm 4 \times 10^{-13}$

* As mentioned in [4].
** As mentioned in [7].

MCM accuracy is strongly dependent on the quality of the tools used to perform the computational work. For the present studies the Mersenne Twister pseudo-random generator [8] was used, being able to generate numerical sequences with a dimension of 10^6 elements, and validated algorithms to perform the probability distributions conversions and the output sorting were used in accordance with [9]. The computational accuracy level of the numerical simulations was achieved using [10].

3.2 Achieved results and sensitivity analysis

The following results presented were obtained from several studies carried out regarding the room-corner test and the radiant panel test, considering the two exposure conditions (displayed on figure 1). Numerical simulations based on MCM were developed in order to obtain measurement uncertainties estimates.

The first set of results is related with the room-corner test, obtained considering that a gaussian PDF describes the probabilistic behaviour of incident radiative heat flux density. Figures 4 to 6 present the 95 % expanded measurement uncertainty with a computational accuracy level lower than ±0,02 $kW \cdot m^{-2}$.

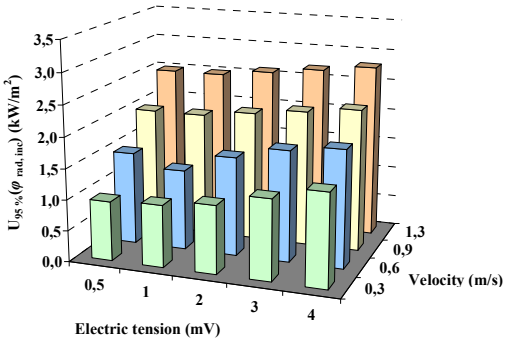

Figure 4. Expanded measurement uncertainties (95 %) for $\hat{T}_\infty = 289$ K .

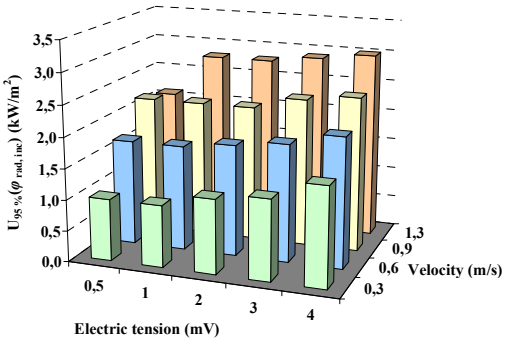

Figure 5. Expanded measurement uncertainties (95 %) for $\hat{T}_\infty = 320$ K .

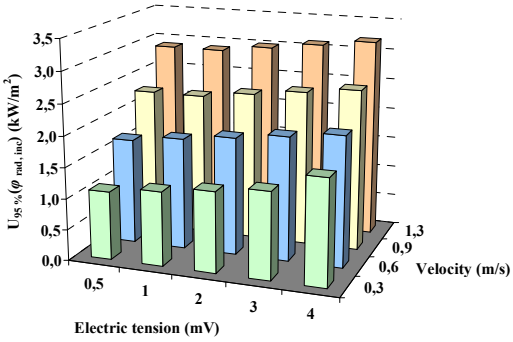

Figure 6. Expanded measurement uncertainties (95 %) for $\hat{T}_\infty = 337$ K .

The results obtained show that the expanded measurement uncertainty of the incident radiative heat flux density quantity can change between ±1,0 kW·m^{-2} to ±3,0 kW·m^{-2} for the measuring interval of 2 kW·m^{-2} to 20 kW·m^{-2} (being the highest value obtained for estimates close to 20 kW·m^{-2}).

In terms of convective effects, it is possible to establish a direct relation between the measurement uncertainty and the air flow velocity in the studied measuring interval. The same effect can be observed for the air flow temperature but with a lower magnitude.

The same probabilistic information as in [4] also provides a comparison between the two uncertainty calculation methods. According with the reference above mentioned "*... an estimated relative uncertainty of 7 % - 25 % when the total heat flux is above 5 kW·m^{-2}. Near flashover conditions, 20 kW·m^{-2}, the relative uncertainty is estimated to be 7 % - 8 %.*". The MCM results are summarized in table 3.

Table 3. Relative standard measurement uncertainties obtained using the MCM.

Incident radiative heat flux density level	Relative standard measurement uncertainty
5 kW·m^{-2}	9 % to 26 %
10 kW·m^{-2}	5 % to 14 %
15 kW·m^{-2}	4 % to 10 %
20 kW·m^{-2}	4 % to 8 %

The relative uncertainty interval predicted by [4] is in good agreement with the results obtained by the MCM for a 5 kW·m^{-2} level. For the remaining levels up to 15 kW·m^{-2}, the relative measurement uncertainty tends to be lower than the solution provided by the GUM method. The same observation can be made for the 20 kW·m^{-2} level, in particular, when considering the lowest estimates for the air flow velocity and temperature.

Figure 7 presents the sensitivity analysis results regarding the expanded measurement uncertainty of the incident radiative heat flux density quantity (for an estimate close to 10 kW·m^{-2}) considering independent increases in input quantity uncertainty contributions.

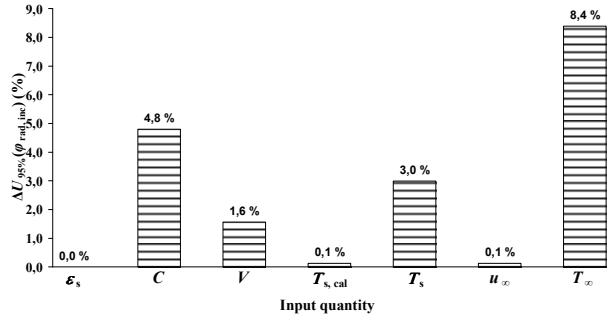

Figure 7. Results of the measurement uncertainty sensitivity analysis (exposure condition 1.a).

The results obtained show that air flow temperature is the most significant contribution to the radiative heat flux density measurement uncertainty. It is followed by the calibration constant, the temperature of the heat flux meter sensor head and the output electric tension. The remaining input quantities have neglectable influence on the output measurement uncertainty. These results are, again, in agreement with the trends found in [4] based on the GUM approach.

Figures 8 to 10 represent the expanded measurement uncertainty (in a 95 % confidence interval) obtained using the MCM for the radiant panel test exposition condition. The shape of the incident radiative heat flux quantity PDF is considered as gaussian for all the input estimates, and the computational accuracy level is below ±0,01 kW·m^{-2}.

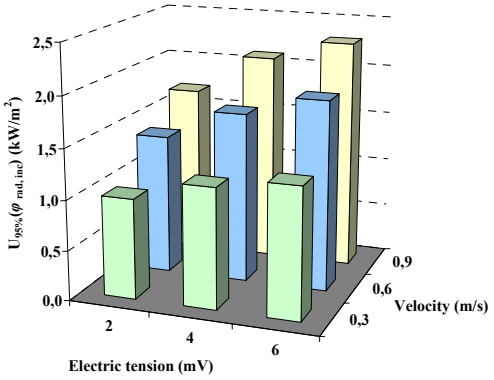

Figure 8. Expanded measurement uncertainties (95 %) for $\hat{T}_\infty = 300$ K .

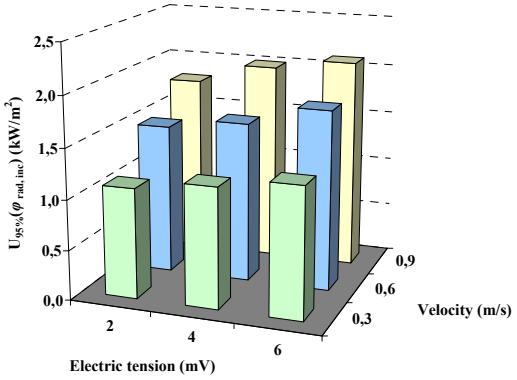

Figure 9. Expanded measurement uncertainties (95 %) for $\hat{T}_\infty = 350$ K .

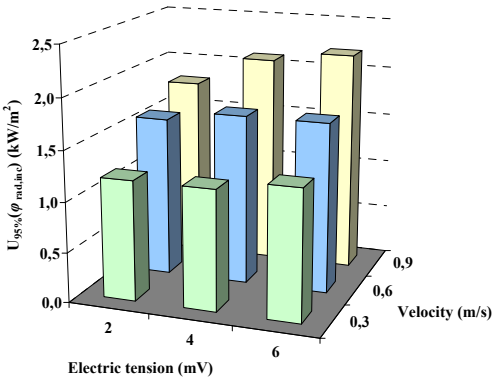

Figure 10. Expanded measurement uncertainties (95 %) for $\hat{T}_\infty = 400$ K .

Although having its own probabilistic framework and mathematical model, the results obtained for the exposure condition in the radiant panel test are similar to the results of the first studied condition. The expanded measurement uncertainty of the incident radiative heat flux density quantity changes between ± 1,0 kW·m^{-2} and ± 2,3 kW·m^{-2}, considering a measuring interval of 2 kW·m^{-2} to 10 kW·m^{-2} (the highest measurement uncertainty occurs when estimates are closer to 10 kW·m^{-2}).

As observed before, the increase of the measurement uncertainty occurs when air flow velocity and temperature are higher, although, in the last case, having lower magnitude.

Figure 11 presents the sensitivity analysis results for the expanded measurement uncertainty variation of the incident radiative heat flux density quantity (for an estimate close to 6 kW·m^{-2}) obtained using a measurement uncertainty increase on influential input quantities.

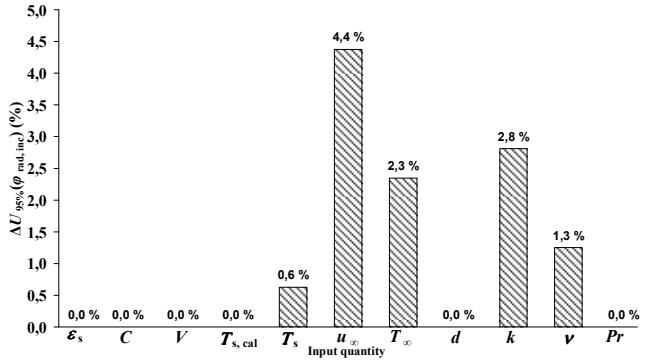

Figure 11. Results of the measurement uncertainty sensitivity analysis (exposure condition 1.b).

The previous figure shows that the air flow velocity has the most significant contribution to the output measurement uncertainty, followed by air thermal conductivity, air flow temperature, cinematic viscosity and temperature of the heat flux meter sensor head. The remaining input quantities have neglectable impact on the output measurement uncertainty.

4. CONCLUSIONS AND FINAL REMARKS

The studies carried out showed how the MCM can provide the incident radiative heat flux density estimate and its measurement uncertainty in reaction to fire tests, taking into account the convective effects created by the heat flux sensor head exposure to the surrounding environmental conditions.

Following the aims presented, the results allows to conclude that, for the exposure condition related with the room-corner test and a measuring range of 2,0 kW·m^{-2} up to 20,0 kW·m^{-2}, the expanded measurement uncertainty found is between ±1,0 kW·m^{-2} and ±3,0 kW·m^{-2}. Regarding the case of the exposure condition in the radiant panel test and a measuring range of 2,0 kW·m^{-2} up to 10,0 kW·m^{-2}, the expanded measurement uncertainty admits values from ±1,0 kW·m^{-2} up to ±2,3 kW·m^{-2}.

The comparison of results related with the first studied exposure condition, although obtained using two different approaches (GUM and MCM), gave similar values, nevertheless, the use of non-linear models makes the use of the MCM more accurate [5] and less complex to implement.

Certain input quantities used had physical constrains that were taken into account on the MCM simulations, as was the case of the air flow velocity (with a large concentration of the PDF near the physical limit of zero) or the surface emissivity (with estimates that can not assume values higher than one). For these cases, alternative approaches, like Bayesian Inference, would be more accurate to apply to this type of probabilistic condition.

The sensitivity analysis shows how different input quantities affect the output accuracy, allowing that the experimental setup can be developed in order to achieve a higher accuracy level. Therefore, improvements to reduce the measurement uncertainty related with the air flow temperature, the calibration constant and the surface temperature in the room-corner test would be the most required. In a similar way, regarding the radiant panel test, improvements would be advisable to reduce measurement uncertainty related with air flow velocity, air flow temperature, surface temperature positively affecting the air thermophysical properties.

REFERENCES

[1] ISO 9705 – *Fire tests – Full-scale room test for surface products*, International Organization for Standardization (ISO), Genève, 1993.

[2] EN ISO 9239-1 – *Reaction to fire tests for floorings – Part 1: Determination of the burnimg behaviour using a radiant heat source*, Comité Européen de Normalisation (CEN), Bruxelles, 2002.

[3] T. E. Diller, "Heat Flux", *The Measurement, Instrumentation and Sensors Handbook*, CRC Press, Boca Raton, 1999.

[4] R. Bryant, C. Womeldorf, E. Johnsson and T. Ohlemiller, "Radiative heat flux measurement uncertainty", *Fire and Materials*, vol. 27, pp. 209 − 222, 2003.

[5] *Evaluation of measurement data − Supplement 1 to the "Guide to the expression of uncertainty in measurement"− Propagation of distributions using a Monte Carlo method*, JCGM, 2008.

[6] F. P. Incropera and D. P. DeWitt, *Fundamentals of Heat and Mass Transfer*, 5th edition, John Wiley & Sons, New York, 2002.

[7] P. J. Mohr, B. N. Taylor and D. B. Newel, "The 2006 CODATA Recommended Values of the Fundamental Physical Constants", web version 5.2, developed by J. Bakeer, M. Douma and S. Kotochigova, National Institute of Standards and Technology (NIST), Gaithersburg, MD (USA), available at http://physics.nist.gov/constants [2009, March 9].

[8] M. Matsumoto and T. Nishimura, "Mersenne Twister: a 623-dimensionally equidistributed uniform pseudorandom number generator", *ACM Transactions on Modelling and Computer Simulations*, vol. 8, nº1, pp. 3-30, January 1998.

[9] W. H. Press. B. P. Flannery, S. A. Teukolsky and W. T. Vetterling, *Numerical recipes – the art of scientific computing*, Cambridge University Press, 1986.

[10] M. G. Cox, M. P. Dainton and P. M. Harris, *Software specifications for uncertainty calculation and associated statistical analysis*, National Physical Laboratory (NPL) report CMSC 10/01, NPL, Teddington, March 2001.